Electronic Supplementary Material (ESI) for Analyst.
This journal is © The Royal Society of Chemistry 2018

Supporting Information For

A dinitro-functionalized metal-organic framework featuring visual and fluorogenic sensing of H_2S in living cells, human blood plasma and environmental samples

Soutick Nandi,[a] *Sooram Banesh,*[b] *Vishal Trivedi,*[b] *and Shyam Biswas**[a]

[a] Department of Chemistry, Indian Institute of Technology Guwahati, Guwahati, 781039 Assam, India

[b] Malaria Research Group, Department of Biosciences and Bioengineering, Indian Institute of Technology Guwahati, 781039 Assam, India

* To whom correspondence should be addressed. E-mail: sbiswas@iitg.ernet.in. Tel: (+)91-3612583309. Fax: (+)91-3612582349.

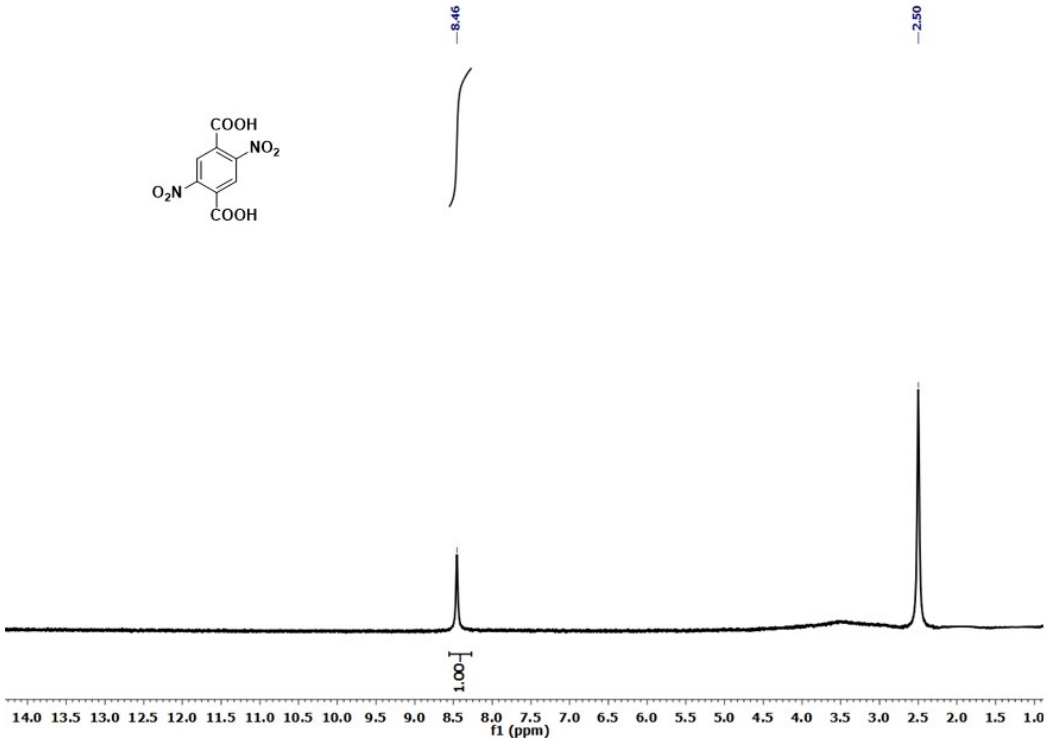

Figure S1. ^{1}H NMR spectrum of $H_2BDC\text{-}(NO_2)_2$ ligand.

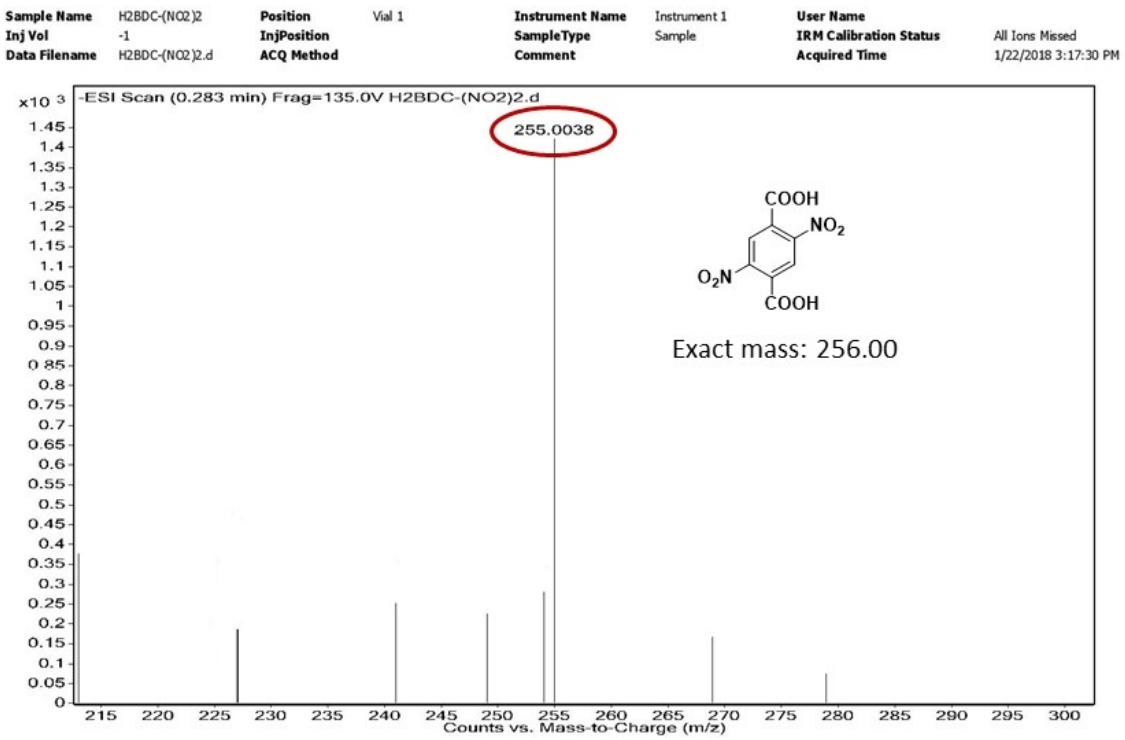

Figure S2. HR-MS spectrum of $H_2BDC\text{-}(NO_2)_2$ ligand.

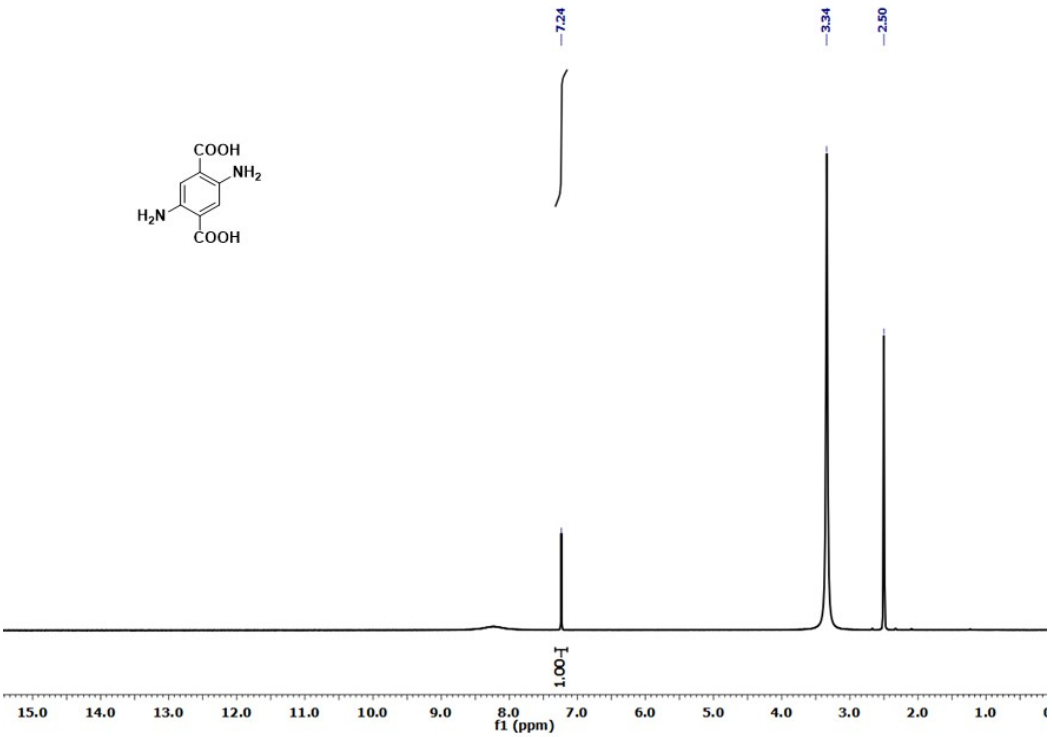

Figure S3. ^{1}H NMR spectrum of $H_2BDC\text{-}(NH_2)_2$ ligand.

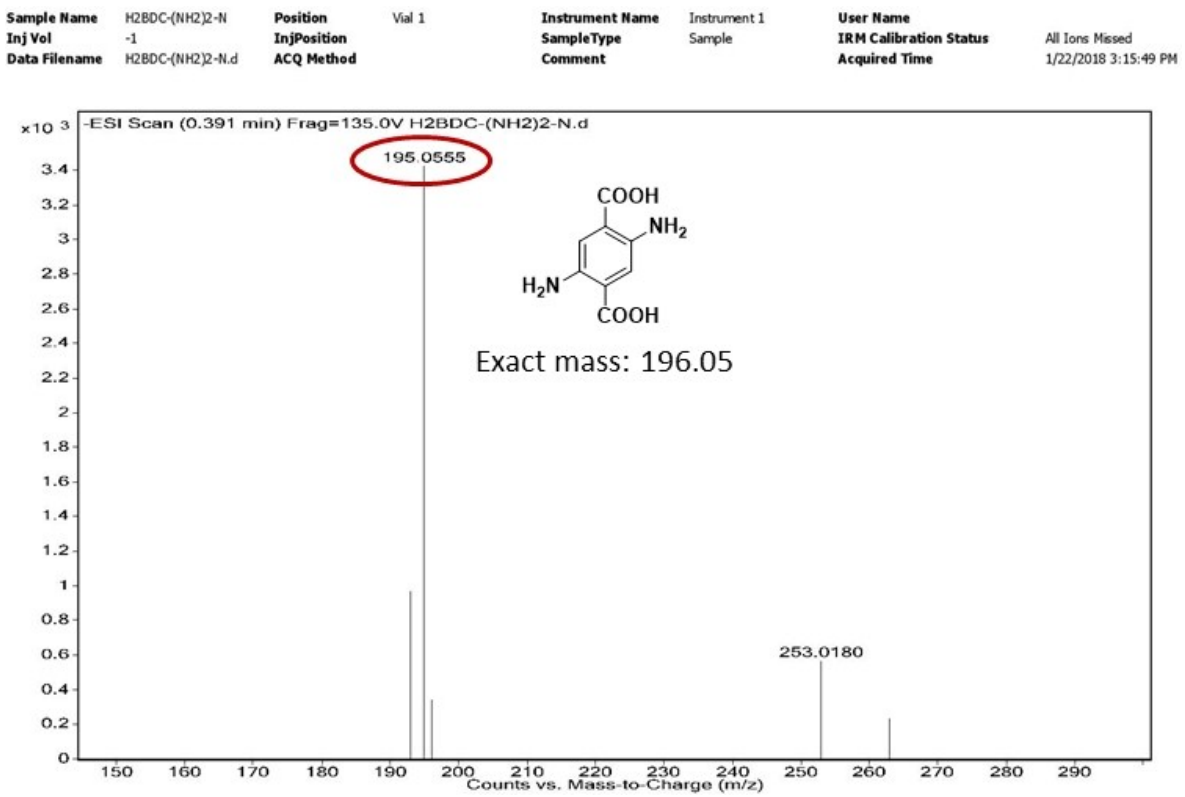

Figure S4. HR-MS spectrum of $H_2BDC\text{-}(NH_2)_2$ ligand.

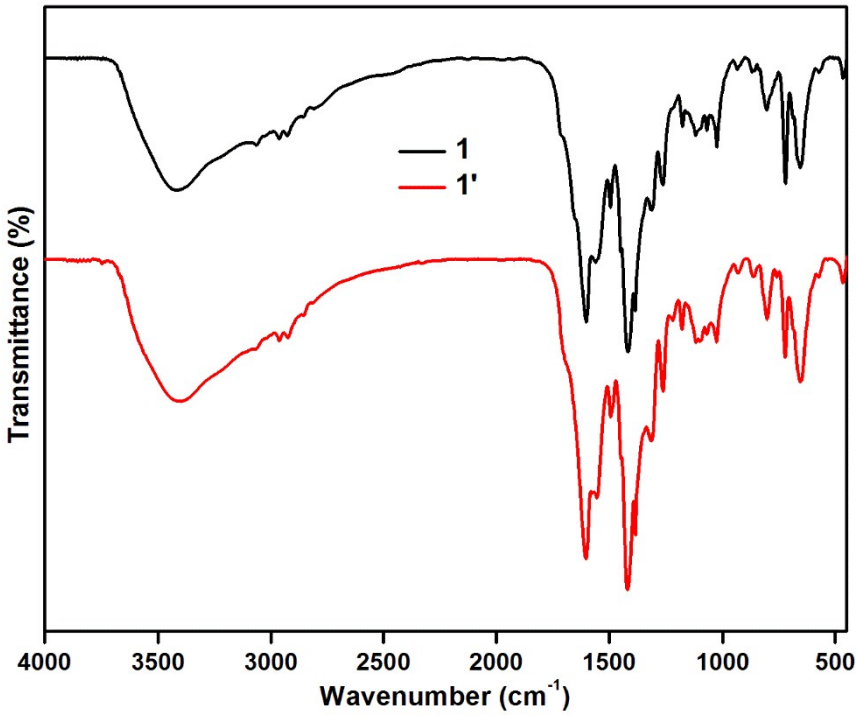

Figure S5. FT-IR spectra of as-synthesized **1** (black) and activated (red) **1'**.

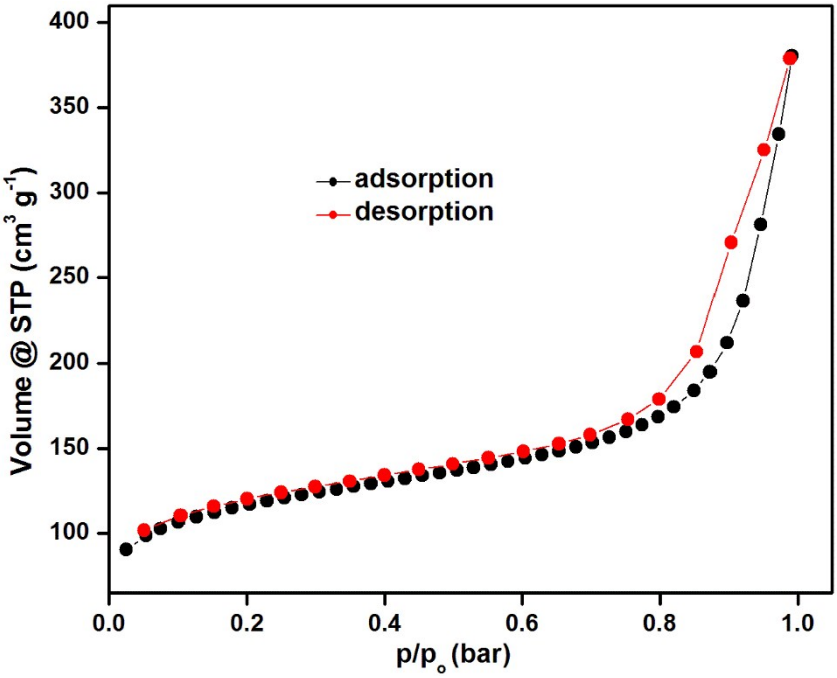

Figure S6. N_2 adsorption (black circles) and desorption (red circles) isotherms of thermally activated **1'** recorded at –196 °C.

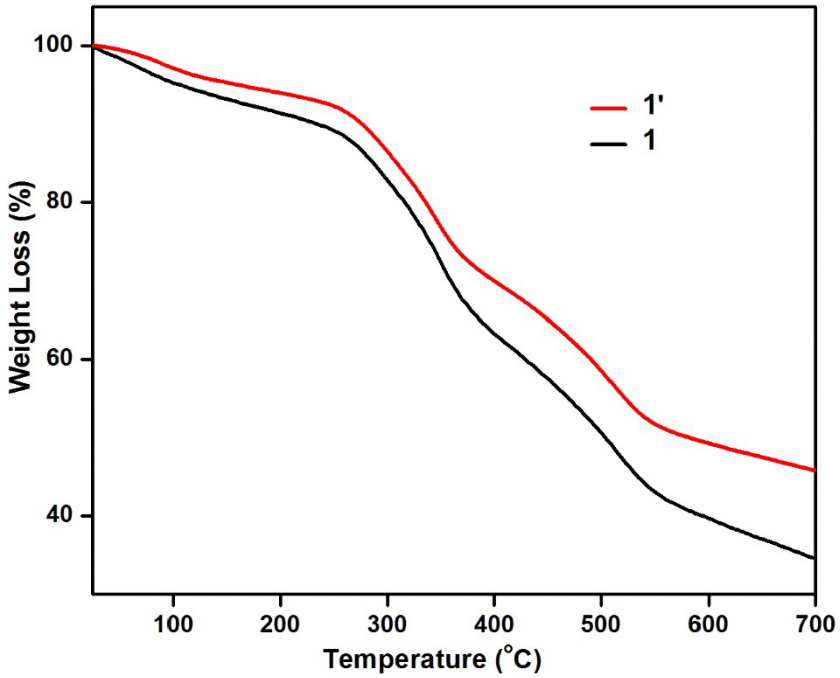

Figure S7. TG curves of as-synthesized **1** (black) and activated **1'** (red) recorded in an air atmosphere in the temperature range of 25-700 °C with a heating rate of 10 °C min^{-1}.

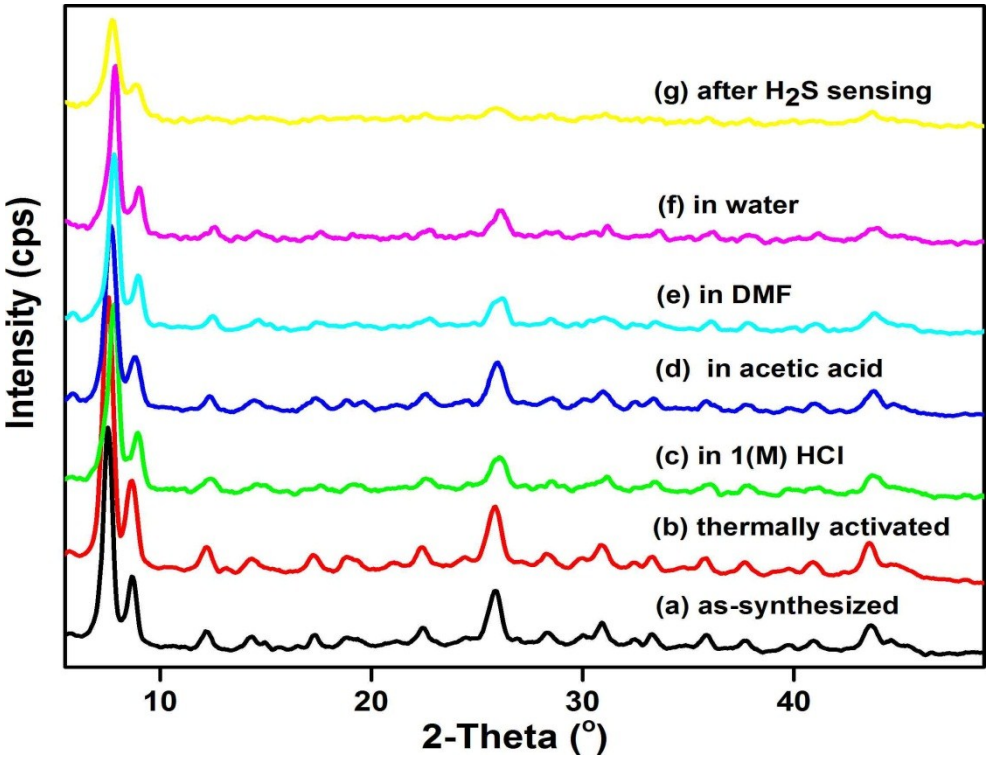

Figure S8. XRPD patterns of **1** in different forms: as-synthesized (a), thermally activated (b), after treatment with 1(M) HCl (c), acetic acid (d), DMF (e), water (f) and after H_2S sensing experiment (g).

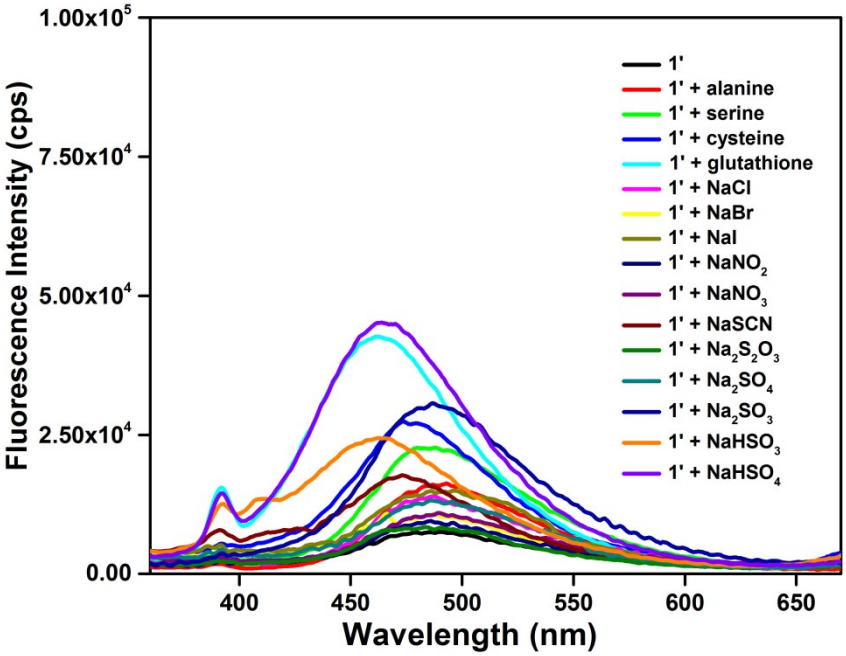

Figure S9. Fluorescence response of **1'** in presence of different analytes.

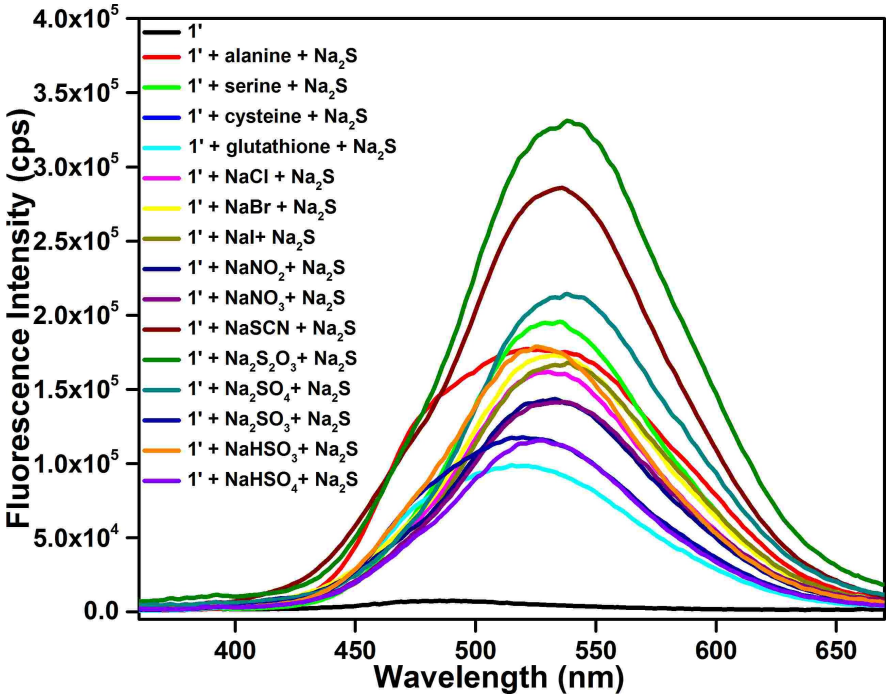

Figure S10. Fluorescence response of **1'** towards H_2S in presence of other interfering analytes.

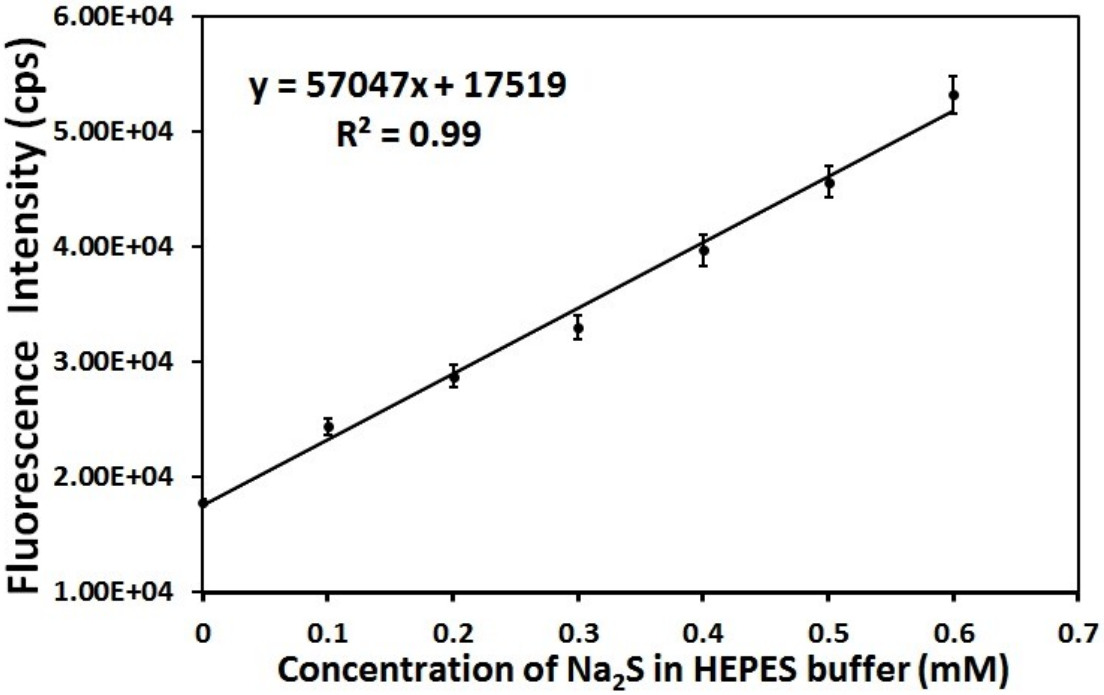

Figure S11. Change in the fluorescence intensity of **1′** in HEPES buffer as a function of Na_2S concentration. The error bars indicate the standard deviations of three measurements.

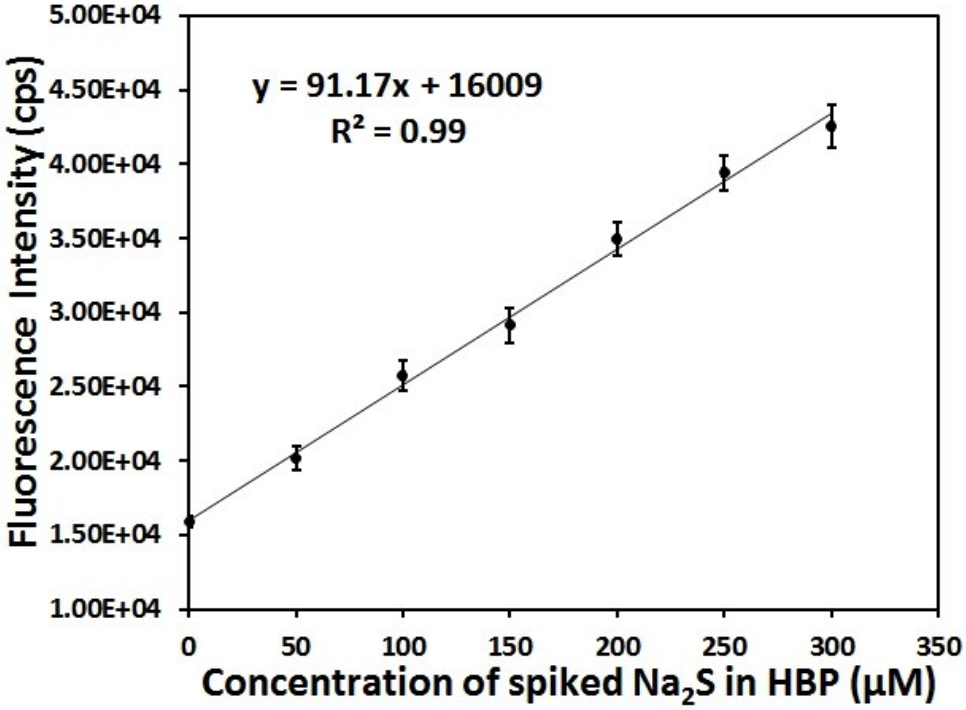

Figure S12. Fluorescence response of **1′** in presence of Na_2S-spiked human blood plasma. Na_2S was spiked as an internal standard. The error bars indicate the standard deviations of three measurements.

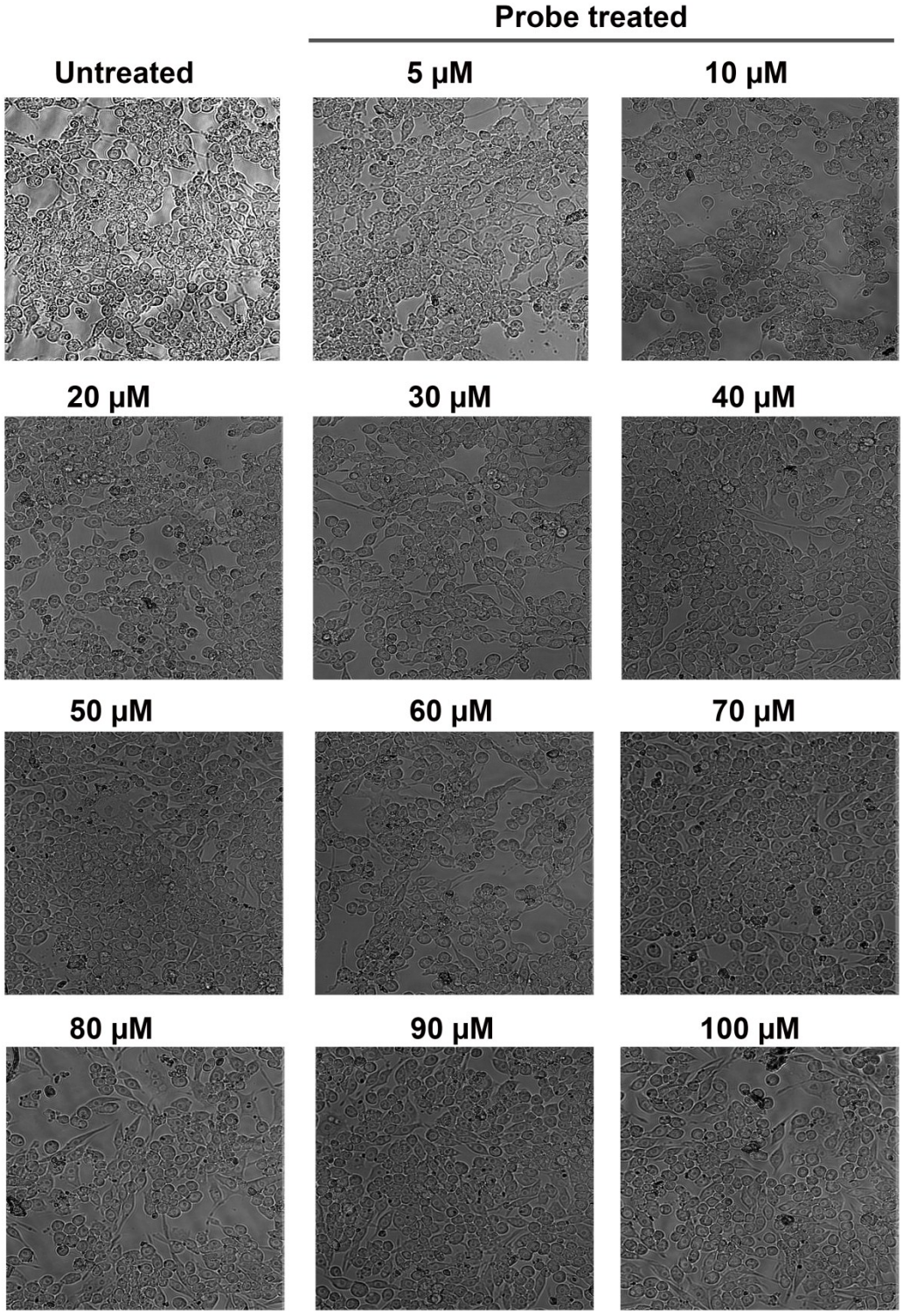

Figure S13. Morphological analysis of **1′**-treated J774A.1 cells. Macrophage J774A.1 cells were treated with different concentrations of probe (0-100 μM) for 24 h at 37 ºC and cells were observed with Cytell cell imaging system (GE Healthcare).

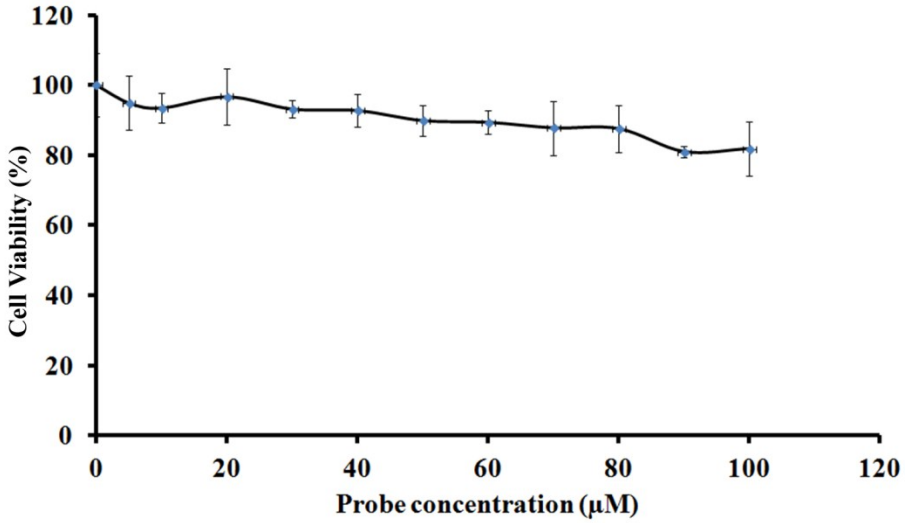

Figure S14. Cytotoxic effect of **1′** on J774A.1 survival. Ten thousand Macrophage J774A.1 cells were treated with different concentrations of probe (0-100 µM) for 24 h at 37 ºC and cellular viability was measured using MTT assay. The cellular viability of untreated cells was considered as 100% to calculate the viability of treated cells. (n=3, $p<0.001$).

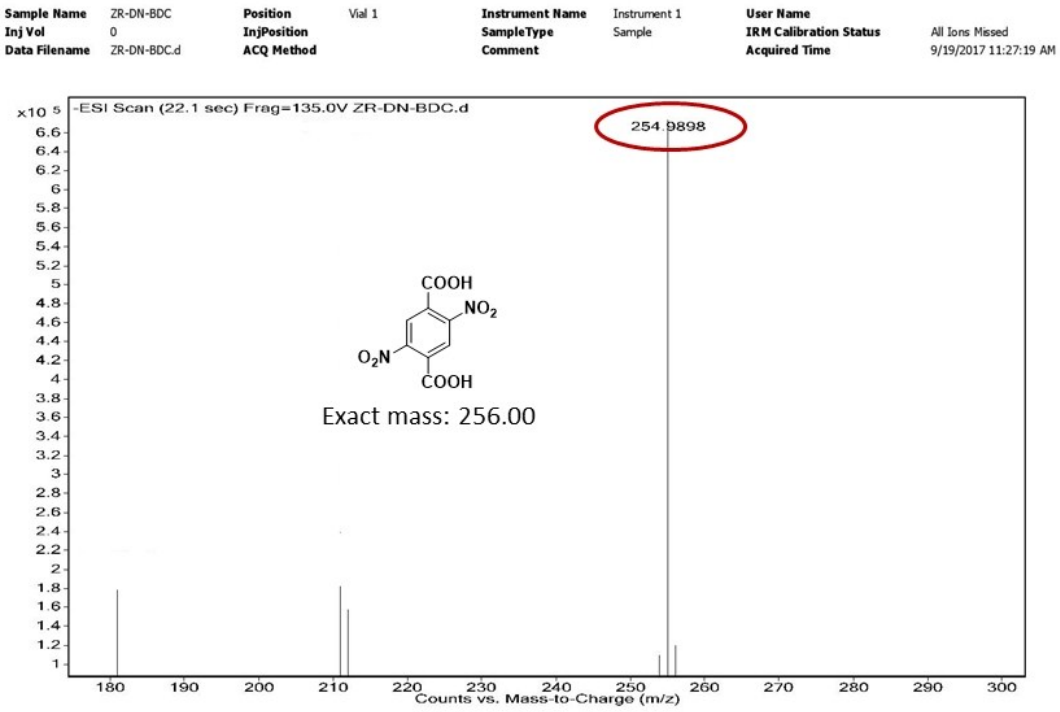

Figure S15. HR-MS spectrum of **1′** (digested in MeOH/HF) showing m/z peak at 254.9898 (negative ion mode), which corresponds to $(M-H)^-$ ion (M = mass of $H_2BDC\text{-}(NO_2)_2$ ligand).

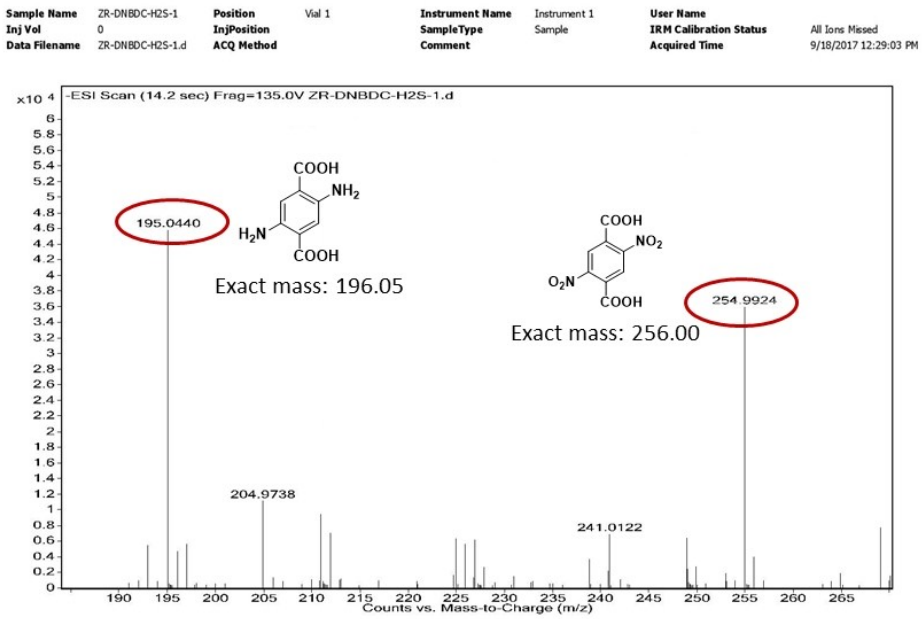

Figure S16. HR-MS spectrum of Na_2S-treated **1′** (digested in MeOH/HF) showing m/z (negative ion mode) peaks at 254.9924 and 195.0440, which correspond to $(M-H)^-$ ion of $H_2BDC\text{-}(NO_2)_2$ ligand and reduced $H_2BDC\text{-}(NO_2)_2$ ligand i.e. $H_2BDC\text{-}(NH_2)_2$, respectively.

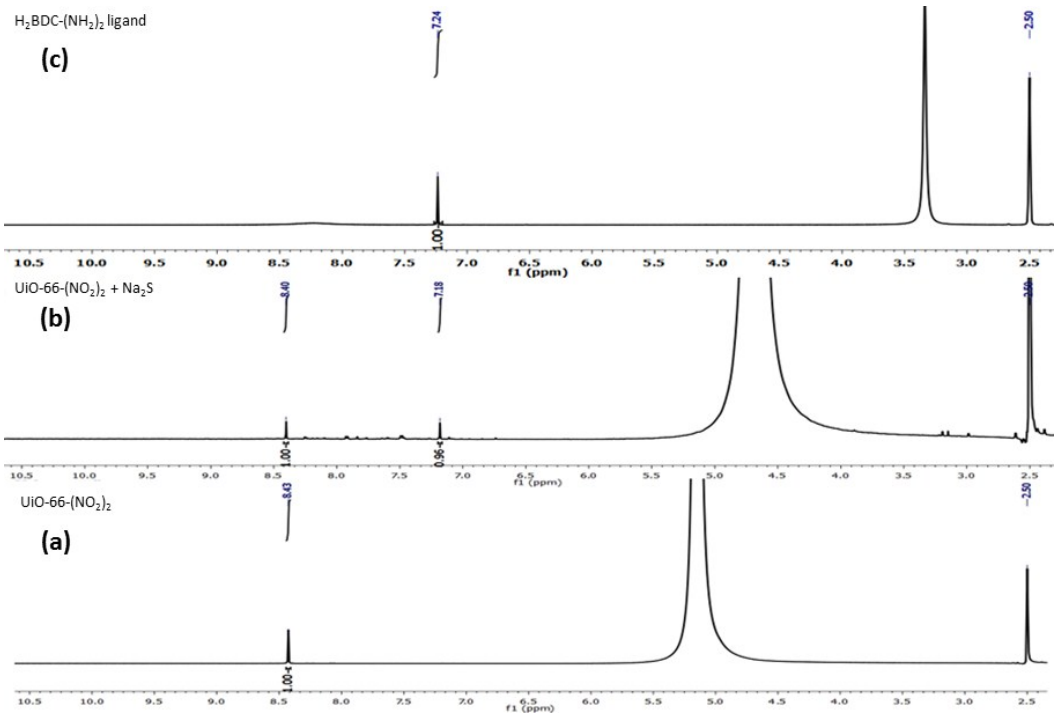

Figure S17. ^{1}H NMR spectra of (a) **1′** (digested in DMSO-d_6/HF), (b) Na_2S-treated **1′** (digested in DMSO-d_6/HF) and (c) H_2BDC-$(NH_2)_2$ ligand (in DMSO-d_6). In the spectrum of Na_2S-treated **1′**, a new peak arises at 7.18 ppm, which closely matches with the peak position (~7.24 ppm) for the aromatic protons of H_2BDC-$(NH_2)_2$ ligand. This observation clearly signifies the formation of the diamine compound i.e. (H_2BDC-$(NH_2)_2$) by reduction of the corresponding dinitro compound (i.e. H_2BDC-$(NO_2)_2$). In order to calculate the percent of conversion from nitro to amine compound, the peak corresponding to the two equivalent aromatic protons of the H_2BDC-$(NO_2)_2$ ligand is set to an integration of 1 and the newly generated peak is integrated accordingly. For Na_2S-treated **1′**, the new peak has an integration value of ~0.96 with respect to the two equivalent aromatic protons of the H_2BDC-$(NO_2)_2$ ligand. Hence, the percentage conversion of nitro to amine compound is ~48%.

Table S1. Comparison of the response time, detection limit and analyte used of various existing probes for the fluorescence detection of H_2S.

Sl. No.	Sensor materials	Type of Material	Response Time (s)	Detection Limit	Analyte	Ref.
1	Zr-UiO-66-$(NO_2)_2$	MOF	2400	14.14 μM	Na_2S	This work
2	DUT-52-$(NO_2)_2$	MOF	3300	20.0 μM	Na_2S	1
3	Ce-UiO-66-N_3	MOF	760	12.2 μM	NaSH	2
4	Ce-UiO-66-NO_2	MOF	760	34.84 μM	NaSH	2
5	CAU-10-N_3	MOF	420	2.65 μM	Na_2S	3
6	IRMOF-3-N_3	MOF	< 120	28.3 μM	NaSH	4
7	Zr-UiO-66-NO_2	MOF	≈ 460	188 μM	Na_2S	5
8	Zr-UiO-66-N_3	MOF	180	118 μM	Na_2S	6
9	MN-ZIF-90	MOF	-	-	-	7
10	Al-TCPP-Cu	MOF	-	-	-	8

11	Al-MIL-101-N_3	MOF	-	100 μM (UV-lamp excitation); 0.1 μM (laser excitation)	Na_2S	9
12	Eu^{3+}/Cu^{2+}@UiO-66-$(COOH)_2$	MOF	30	5.45 μM	NaSH	10
13	NHS1	organic molecule	4800	20 nM	NaSH	11
14	Cy-N_3	organic molecule	1200	0.08 μM	NaSH	12
15	SFP-1, SFP-2	organic molecule	7200, 14400	-	Na_2S	13
16	SHS-M1, SHS-M2	organic molecule	-	0.2 μM, 0.4 μM	Na_2S	14
17	probe 1	organic molecule	≈ 3600	2.4 μM	NaSH	15
18	SF4	organic molecule	-	125 nM	NaSH	16
19	WSP5	organic molecule	-	47 nM	NaSH	17
20	NIR-H_2S	organic molecule	-	5×10^{-8} M	NaSH	18
21	probe 1	organic molecule	10800	-	Na_2S	19
22	Cy–NO_2	organic molecule	5400	2 μM	Na_2S	20
23	probe 1	organic molecule	2700	2.5 μM	Na_2S	21
24	RHP-2	organic molecule	2400	270 nM	Na_2S	22
25	HSN1, HSN2	organic molecule	5400, 2700	5-10 μM, 1-5 μM	H_2S	23
26	FS1	organic molecule	7200	5-10 μM	Na_2S	24
27	PI-N_3	organic molecule	180	8.79×10^{-7} M	NaSH	25
28	Probe 1	organic molecule	1800	3.05 μM	NaSH	26
29	Probe 1	organic molecule	180-600	0.78 nM	NaSH	27
30	Probe 4	organic molecule	600	259 nM	Na_2S	28
31	Probe 1	organic molecule	180	0.13 μM	NaSH	29
32	TPE-Az	organic molecule	120	-	NaSH	30
33	AzMB-coumarin	organic molecule	1200-2400	100 μM	NaSH	31

34	Lyso-AFP	organic molecule	1800	-	NaSH	32
35	SF1, SF2	organic molecule	3600	5-10 μM	NaSH	33
36	cpGFP-Tyr66pAzF	organic molecule	420	-	NaSH	34
37	CLSS-1, CLSS-2	organic molecule	-	0.7 ± 0.3 μM, 4.6 ± 2.0 μM	NaSH	35
38	DNS-Az	organic molecule	-	1 μM	Na_2S	36

Quantum yield measurement:

Quantum yield is defined as a ratio of the number of emitted photons from a sample as fluorescence to the number of photons absorbed from the excited light. The fluorescence quantum yield of the Na_2S-treated UiO-66-$(NO_2)_2$ (**1′**) was evaluated by Parker-Rees method[37] using quinine sulphate (in 0.5 M H_2SO_4) as a standard fluorophore. The Parker-Rees equation can be written as follows:

$$\phi_u = (A_s F_u n_u^2 / A_u F_s n_s^2)\, \phi_s \qquad (1)$$

where ϕ_s is the quantum yield of the reference (quinine sulphate, 0.54) in 0.5 M H_2SO_4, ϕ_u is the quantum yield of Na_2S-treated **1′** in HEPES buffer medium, A_s and A_u are the absorbances of quinine sulphate and Na_2S-treated **1′** at the excitation wave-length (345 nm), respectively. To minimize the reabsorption of the fluorescence light passing through the samples, their absorbance maxima were kept less than 0.1. F_s and F_u are the areas of integrated fluorescence intensity of the quinine sulphate and Na_2S-treated **1′** when excited at the same excitation wavelength, respectively. The refractive indices of the solvents for sample and quinine sulphate are denoted by n_u and n_s, respectively (both are water-based medium, so $n_u = n_s$). The obtained quantum yield according to equation (**1**) for Na_2S-treated UiO-66-$(NO_2)_2$ (i.e. UiO-66-$(NH_2)_2$) is 0.04."

Table S2. Photo-physical parameters of Na_2S-treated UiO-66-$(NO_2)_2$ (i.e. UiO-66-$(NH_2)_2$).

Sl. No.	Sample Name	Excitation Wavelength λ_{ex} (nm)	Absorbance (A)	Area of Integrated Fluorescence Intensity (F)	Quantum Yield **(ϕ)**
1	Quinine Sulphate	345	0.081	6.02×10^8	0.54
2	UiO-66-$(NH_2)_2$	345	0.058	3.14×10^7	0.04

References:

1. R. Dalapati, S. N. Balaji, V. Trivedi, L. Khamari and S. Biswas, *Sens. Actuators., B*, 2017, **245**, 1039-1049.
2. A. Buragohain and S. Biswas, *CrystEngComm*, 2016, **18**, 4374-4381.
3. S. Nandi, H. Reinsch, S. Banesh, N. Stock, V. Trivedi and S. Biswas, *Dalton Trans.*, 2017, **46**, 12856-12864.
4. X. Zhang, J. Zhang, Q. Hu, Y. Cui, Y. Yang and G. Qian, *Appl. Surf. Sci.*, 2015, **355**, 814.
5. S. S. Nagarkar, A. V. Desai and S. K. Ghosh, *Chem. Eur. J.*, 2015, **21**, 9994-9997.
6. S. S. Nagarkar, T. Saha, A. V. Desai, P. Talukdar and S. K. Ghosh, *Sci. Rep.*, 2014, **4**, 7053-7058.
7. H. Li, X. Feng, Y. Guo, D. Chen, R. Li, X. Ren, X. Jiang, Y. Dong and B. Wang, *Sci. Rep.*, 2014, **4**, 4366-4370.
8. Y. Ma, H. Su, X. Kuang, X. Li, T. Zhang and B. Tang, *Anal. Chem.*, 2014, **86**, 11459-11463.
9. A. Legrand, A. Pastushenko, V. Lysenko, A. Geloen, E. A. Quadrelli, J. Canivet and D. Farrusseng, *ChemNanoMat*, 2016, **2**, 866-872.
10. X. Zhang, Q. Hu, T. Xia, J. Zhang, Y. Yang, Y. Cui, B. Chen and G. Qian, *ACS Appl. Mater. Interfaces*, 2016, **8**, 32259–32265.
11. G.-J. Mao, T.-T. Wei, X.-X. Wang, S.-y. Huan, D.-Q. Lu, J. Zhang, X.-B. Zhang, W. Tan, G.-L. Shen and R.-Q. Yu, *Anal. Chem.*, 2013, **85**, 7875-7881.
12. F. Yu, P. Li, P. Song, B. Wang, J. Zhao and K. Han, *Chem. Commun.*, 2012, **48**, 2852-2854.
13. Y. Qian, J. Karpus, O. Kabil, S.-Y. Zhang, H.-L. Zhu, R. Banerjee, J. Zhao and C. He, *Nat. Commun.*, 2011, **2**, 495.
14. S. K. Bae, C. H. Heo, D. J. Choi, D. Sen, E.-H. Joe, B. R. Cho and H. M. Kim, *J. Am. Chem. Soc.*, 2013, **135**, 9915-9923.
15. Y. Jiang, Q. Wu and X. Chang, *Talanta*, 2014, **121**, 122-126.
16. V. S. Lin, A. R. Lippert and C. J. Chang, *Proc. Natl. Acad. Sci. U.S.A.*, 2013, **110**, 7131-7135.
17. B. Peng, W. Chen, C. Liu, E. W. Rosser, A. Pacheco, Y. Zhao, H. C. Aguilar and M. Xian, *Chem. Eur. J.*, 2013, **20**, 1010-1016.
18. X. Cao, W. Lin, K. Zheng and L. He, *Chem. Commun.*, 2012, **48**, 10529–10531.
19. W. Xuan, R. Pan, Y. Cao, K. Liu and W. Wang, *Chem. Commun.*, 2012, **48**, 10669–10671.
20. R. Wang, F. Yu, L. Chen, H. Chen, L. Wang and W. Zhang, *Chem. Commun.*, 2012, **48**, 11757–11759.
21. M.-Y. Wu, K. Li, J.-T. Hou, Z. Huang and X.-Q. Yu, *Org. Biomol. Chem.*, 2012, **10**, 8342-8347.
22. L. Zhang, W. G. Meng, L. Lu, Y. S. Xue, C. Li, F. Zou, Y. Liu and J. Zhao, *Sci. Rep.*, 2014, **29**, 5870.
23. L. A. Montoya and M. D. Pluth, *Chem. Commun.*, 2012, **48**, 4767–4769.
24. S. K. Das, C. S. Lim, S. Y. Yang, J. H. Han and B. R. Cho, *Chem. Commun.*, 2012, **48**, 8395–8397.
25. K. Zheng, W. Lin and L. Tan, *Org. Biomol. Chem.*, 2012, **10**, 9683–9688.
26. W. Sun, J. Fan, C. Hu, J. Cao, H. Zhang, X. Xiong, J. Wang, S. Cui, S. Sun and X. Peng, *Chem. Commun.*, 2013, **49**, 3890-3892.
27. J. Zhang and W. Guo, *Chem. Commun.*, 2014, **50**, 4214-4217.
28. T. Saha, D. Kand and P. Talukdar, *Org. Biomol. Chem.*, 2013, **11**, 8166–8170.
29. Y. Liu and G. Feng, *Org. Biomol. Chem.*, 2014, **12**, 438–445.

30. Y. Cai, L. Li, Z. Wang, J. Z. Sun, A. Qin and B. Z. Tang, *Chem. Commun.*, 2014, **50**, 8892-8895.
31. Z. Wu, Z. Li, L. Yang, J. Han and S. Han, *Chem. Commun.*, 2012, **48**, 10120–10122.
32. Q. Qiao, M. Zhao, H. Lang, D. Mao, J. Cui and Z. Xu, *RSC Adv.*, 2014, **4**, 25790-25794.
33. A. R. Lippert, E. J. New and C. J. Chang, *J. Am. Chem. Soc.*, 2011, **133**, 10078–10080.
34. S. Chen, Z.-j. Chen, W. Ren and H.-w. Ai, *J. Am. Chem. Soc.*, 2012, **134**, 9589−9592.
35. T. S. Bailey and M. D. Pluth, *J. Am. Chem. Soc.*, 2013, **135**, 16697−16704.
36. H. Peng, Y. Cheng, C. Dai, A. L. King, B. L. Predmore, D. J. Leferand and B. Wang, *Angew. Chem. Int. Ed.*, 2011, **50**, 9672 –9675.
37. C. A. Parker and W. T. Rees, *Analyst*, 1960, **85**, 587-600.